OBSERVATIONS OF THE MARS YEAR 35 E (EARLY) LARGE-SCALE REGIONAL DUST EVENT

D. M. Kass, A. Kleinböhl, *Jet Propulsion Laboratory/California Institute of Technology, Pasadena, USA (David.M.Kass@jpl.nasa.gov)*, **J. Shirley,** *TORQUEFX, Simi Valley, USA,* **B. A. Cantor**, *Malin Space Science System, San Diego, USA,* **N. G. Heavens**, *Space Science Institute, Boulder, USA and London, UK.*

Introduction:

In Mars Year 35 a large-scale regional dust event started at Ls ~ 35° and lasted until Ls ~ 50°. This is during northern spring when interannual variability is usually low and generally only local and small regional dust events occur. This absence of large dust events makes this season attractive for landing spacecraft on Mars, so an unusually large dust event at this season is of interest for forecasting weather conditions for future landings. We designate the event as the MY 35 E (for early) large-scale dust event to distinguish it from the traditional perihelion season A, B and C events as well as late northern summer Z events [1, 2]. We use a combination of MARCI [3] and MCS [4] observations to examine the context, development and evolution of this unusual dust event.

The Typical Northern Spring Season:

The northern spring (early part of the aphelion season) is generally a cold, cloudy and relatively dust free season. The seasonal behavior is partly driven by Mars approaching aphelion (Ls = 71°) and thus it is relatively far from the sun which and reduces the amount of heating. Figure 1 shows the relatively cold temperatures of the northern spring season. In most years, the weather is limited and the atmosphere strongly resembles the median behavior. The atmosphere is dominated by the aphelion water ice cloud belt [5] that forms in the tropics shortly after the start of the season. The clouds are particularly prominent over the highest of the volcanoes, especially Olympus Mons, the Tharsis Montes, Alba Patera and Elysium Mons (Figure 2).
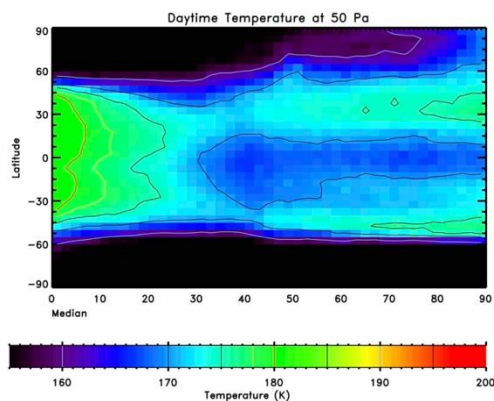

Figure 1: Median zonal mean temperature at 50 Pa (~25 km) for northern spring season from MCS. The median is calculated across MY 29 through MY 35.

During the northern spring, the global atmospheric circulation transitions from an equinoctial two cell system to a solstitial single cross equatorial cell with the upwelling branch in the northern hemisphere and downwelling around the southern polar vortex. This transition is also associated with the disappearance of the northern polar vortex.

MARCI Observations:

MARCI daily global maps record the initiation, development and growth of the MY 35 E event. Figure 2 shows from May 31, 2019 (Ls = 32.8°) the initiation of the event as a textured local dust storm northwest of Olympus Mons (indicated by the red arrow). This is a common location for textured local dust storms to form, but not normally at this season [6]. Otherwise, the weather on this sol is typical for the season with thick (white) water ice clouds crowning all of the volcanoes (the green arrow points to the one over Alba Patera). The general aphelion cloud belt is also visible as a light blue-white haze over the tropics (most noticeable over the darker terrains).

Over the next four days (through June 4th, Ls = 34.6°), the local dust storm expanded into a regional dust storm. It primarily expanded towards the east-northeast, basically in the direction of Alba Patera and then beyond. By June 4th, it was latitudinally still fairly narrow (no more than 30° wide in latitude), but extended almost to 300° East. By this point, the dust was clearly interacting with the mountain flow around Alba Patera. The dust still remained primarily to the north of the volcano. The clouds crowning the volcano had essentially disappeared, although the volcano itself was still visible.

On the following day (June 5th, Ls = 35.1°, not shown), the dust started to expand southward towards the Tharsis plateau. The largest southward expansion of the dust was to the south of Alba Patera. The volcano also became indistinct, indicating that dust was being lofted well above its top—possibly due to being entrained in the anabatic flows (up-slope daytime flows). The dust also expanded another ~15° east in longitude. It is unclear if this was just dust advected from the lifting centers or if there was an expansion of the active lifting regions.

Four days later (June 9th, Ls = 36.9°), the dust reached its maximum visible extent (Figure 3). The dust (outlined by the red arrows in Figure 3) now extended well onto the Tharsis plateau as well as

surrounding Olympus Mons and almost reaching Ascraeus Mons (the northernmost of the Tharsis Montes). The eastern extension of the dust had contracted back to the west and now did not extend beyond ~285° East. This day marked the end of the dust lifting associated with the event. Also, by this time, the clouds above Olympus Mon disappeared as they did earlier over Alba Patera (green star) while those above the Tharsis Montes were very thin.

Over the next several days, the dust abated in the visible imagery as the thick dust in the boundary layer sedimented back onto the surface. However, the atmosphere was still quite hazy, with noticeably more dust than usual for the season.

MCS Observations:

MCS acquired observations of the MY 35 E large-scale regional dust event, providing vertical profiles of temperature, dust and water ice in the atmosphere throughout its lifetime [7-9]. MCS observations are also used to determine dust and water ice column opacities [10]. The observations clearly show the development and evolution of a large-scale regional dust event with a temperature response ultimately affecting most of the atmosphere. By the time the event initiated, the atmosphere had mostly transitioned into the solstitial single cell circulation. The circulation at the time was upwelling in the north and the reverse of what it usually is during
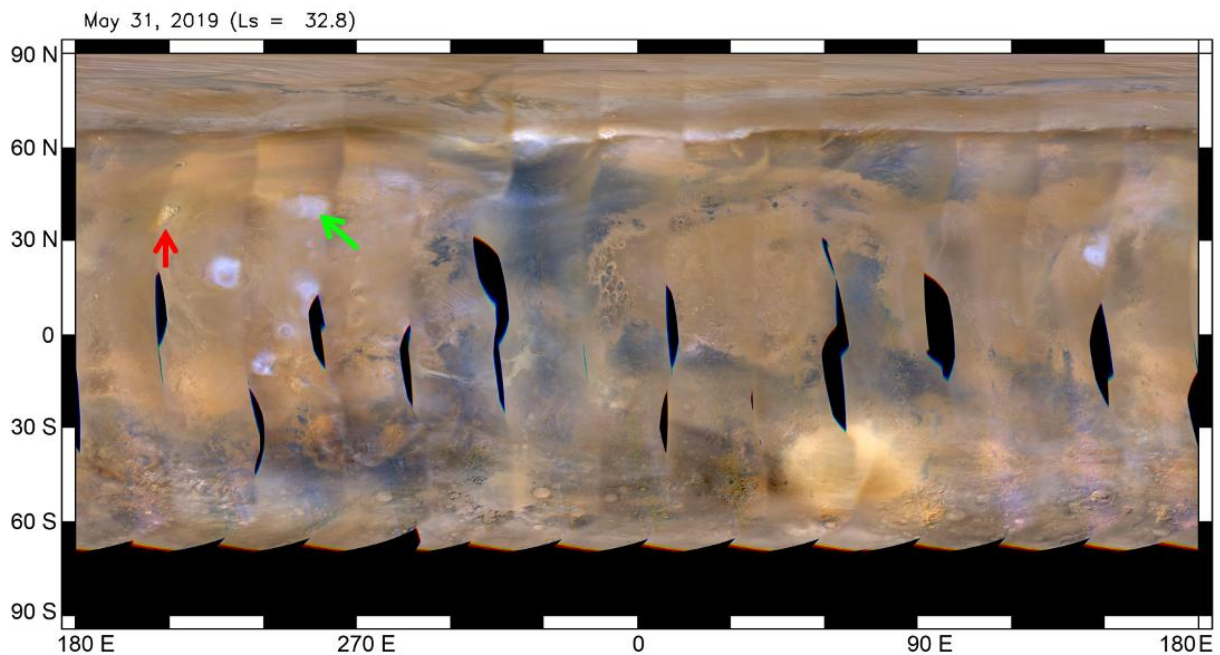

Figure 2: MARCI daily global map for May 31, 2019 (Ls = 32.8°). This is the sol when the large-scale regional dust event initiated. The red arrow points to the initial local dust storm. The green arrow points to the water ice clouds above Alba Patera.
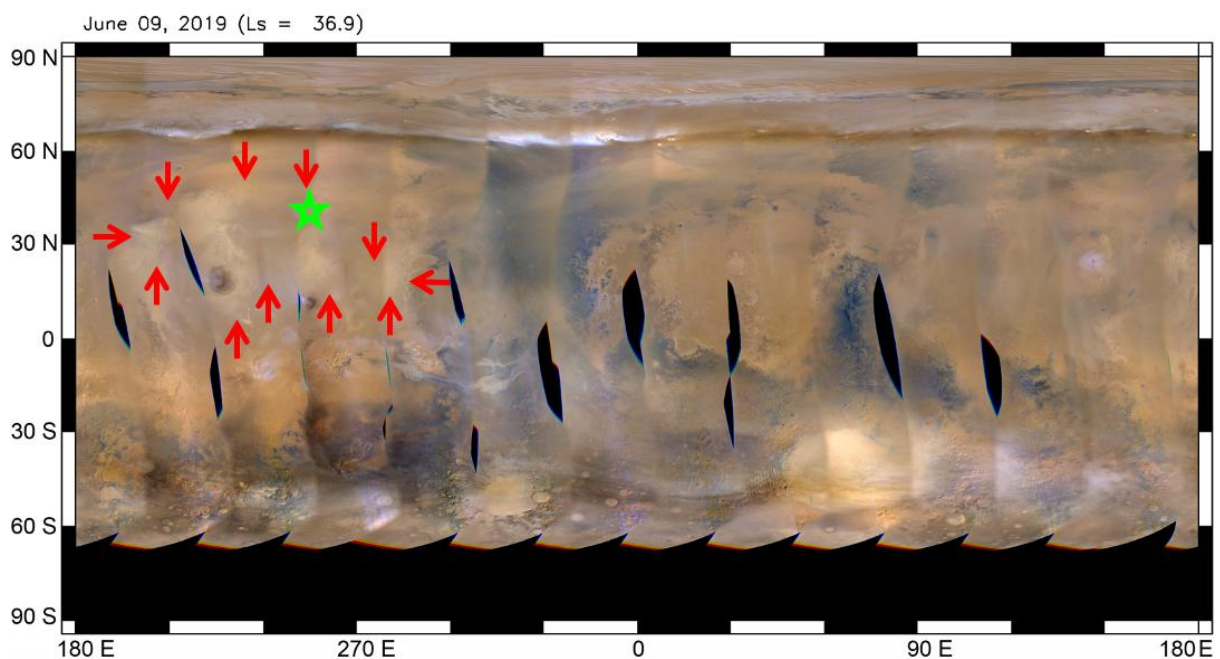

Figure 3: MARCI daily global map for June 9, 2019 (Ls = 36.9°), the peak extent of the event in the visible imagery. The red arrows outline the dust cloud. The green star indicates the location of Alba Patera.

large-scale regional dust events due to the different season.

At 50 Pa (~25 km i.e., well above the boundary layer) in the daytime temperature, the initial signature of the event is a very subtle change on June 3rd (Ls = 34.2°). This is primarily a modest warming of a region centered around 270° E and 50° N— basically a northern extension of the mid-latitude warm region. The first clear signature is not until two days later (June 5th, Ls = 35.1°). That day shows a clear warming (~5 K) centered around 270° E and 40° N, or close to Alba Patera. This matches the time when the MARCI images clearly show signatures of dust lofting around the volcano. The next day shows the first hint of a dynamical response in the southern mid latitudes in the descending branch of the overturning circulation. Over the following days (by June 9, Ls = 36.9°), the 50 Pa response had significantly strengthened (with temperature increases of ~15 K) and, at least in the north, the warming spread to all longitudes. The event continued to produce increasing temperatures at 50 Pa for almost another week.
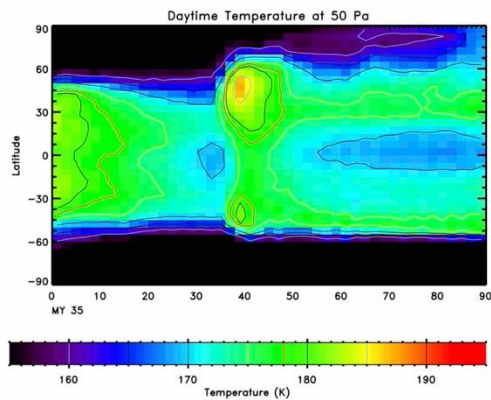

Figure 4: Zonal mean temperature at 50 Pa (~25 km) for the MY 35 northern spring season.
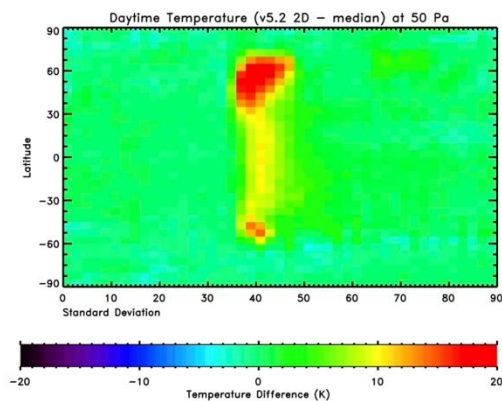

Figure 5: Difference in the zonal mean 50 Pa temperatures between MY 35 and the Median (MY 35 – median), indicating the dust event's perturbation.

The zonal mean 50 Pa daytime temperatures responded quite strongly to the MY 35 E event (Figures 4 and 5). Comparing figures 1 and 4 shows the strong impact that the event had on a normally quiet and cold season. Figure 5 shows the difference between MY 35 and the median year. The northern (or primary) warming reached zonal mean temperatures of almost 20 K above the seasonal values. The southern warming was not as strong, but still reached temperatures ~15 K above the seasonally expected values. Both the north and south temperatures peaked at Ls ~ 39°.

The MY 35 E event also shows up clearly in the dust and water ice fields. The dust column shows strong development and elevated dust in the vicinity of Alba Patera, extending as far as the equator and 60° N. A relatively thin dust haze was detectable at all longitudes in the latter part of the event. Initially, there was only a modest increase in dust in the southern hemisphere, just outside the vortex— presumably a small amount transported south by the overturning circulation. However, dust did start to appear in the southern tropics at Ls ~ 40° and eventually extended as far as 40° S. As seen in the MARCI images, the water ice of the aphelion cloud belt was significantly reduced during the growth stages of the event, through Ls ~ 40°. The ice did reappear afterwards and rapidly returned to the seasonally expected opacity and latitudinal coverage.

Comparison to "C" Events:

In some ways, the MY 35 E large-scale regional dust event is similar to C events that occur after the solstice in the perihelion season (it also shares some similarities with the A events), with an expected north/south swap due to the location of the sub-solar point and the direction of the circulation. In all these events, there is a direct heating (and the primary dust lifting and lofting) in the "sunny" (spring or summer) hemisphere with a strong dynamical response in the opposite hemisphere in the descending branch of the overturning circulation. The overall temperature response indicates an enhancement in the thermal tides in both cases. Likewise, the duration of the E and C events is similar at ~15° of Ls. Another similarity is the relatively modest fall/winter hemisphere dynamical response with usually a short duration—often shorter than the primary warming in C events as seen in the E event. One noticeable difference is the peak warming (in the 50 Pa zonal mean temperature) relative to the "background" conditions. The E event had ~20 K of warming. Some C events only have 15 K to 20 K of warming, but most have > 30 K with the strongest exceeding 35 K of warming. This is not surprising since the sun is further from Mars (and thus solar irradiance is much lower) at the season of the E event. Another difference was that in C events, the initiating local/regional dust storm forms in the winter (northern) hemisphere and travels down one of the cross-equatorial dust storm tracks [11]. Overall, it is very likely that similar dynamical forcing and responses are triggered by both the E and the C events (and

probably the A events) despite the large seasonal differences in the atmosphere.

Discussion:
The appearance of a seasonally atypical local dust storm NW of Olympus Mons might indicate there was very strong northern hemisphere baroclinic activity for the season in MY 35. While there are northern hemisphere local dust storms at this season, they tend to be polar ones [12, 13] and thus may not interact with Alba Patera. The ruffled textured structure is indicative of convective rolls in the initial dust lifting. The orientation of the convective rolls is indicative of an east-west wind in the region and the initial transport of the dust to the east indicates it was a strong westerly flow that triggered the event and governed its initial growth and spread.

It is clear that a key event in the evolution of the dust storm was the interaction with Alba Patera, presumably through mesoscale volcano driven winds. In particular, the interactions with Alba Patera are what drove the event from a medium sized regional dust storm into a full large-scale regional dust event that affected the thermal structure nearly globally. It is unclear if without the assistance of Alba Patera anabatic flows (plus possibly those of Olympus Mons later in the event) the storm would have lofted the necessary amount of dust well above the boundary layer into the lower atmosphere. However, it is not certain that only the interaction with mountain circulations caused the transition since dusty deep convection is seen over Olympus Mons and the Tharsis Montes at seasons without large scale regional dust events (although this is usually after then northern solstice) [2, 14]. It is interesting to consider if Alba Patera modified flows were a large part of initially driving the dust south and up onto the Tharsis ridge (perhaps katabatic flows rapidly transported some of the dust from above/on the southern flanks south overnight on June 4th/5th). It is probable that interactions with the mesoscale circulations around Tharsis, the Tharsis Montes, and Olympus Mons also played an important role in the later evolution of the dust event.

It is interesting to note that the MY 35 E event occurred shortly after the MY 34 global dust event. However, it must be remembered that there was also a strong MY 34 C large-scale regional dust event between the two [15]. Still, one has to ask the question of whether there was an unusual dust distribution that allow the initiation of the dust storm or allowed it to grow to regional scale. Likewise, one may ask whether some residual effect from the MY 34 global dust event led to an unseasonably strong circulation that might be able to initiate such an unexpected local dust storm.

References:
[1] Kass, D. M. et al. (2016) GRL, 43(12), doi: 10.1002/2016GL068978.
[2] Heavens, N. G. et al. (2019) JAS, 76(11), doi: 10.1175/JAS-D-19-0042.1
[3] Bell, J. F. et al. (2009) JGR, 114, E08S92, doi: 10.1029/2008JE003315
[4] McCleese, D. J. et al. (2007) JGR, 112, E05S06.
[5] Clancy et al., ACB
[6] Heavens, N. G. (2017), JAS, 74(4), doi: 10.1175/JAS-D-16-0211.1
[7] Kleinböhl, A. et al. (2009) JGR, 114, E10006.
[8] Kleinböhl, A. et al. (2011) JQSRT, 112, 1568-1580.
[9] Kleinböhl, A. et al. (2017) JQSRT, 112, 511-522.
[10] Kleinböhl, A. et al. (2022) Seventh Workshop on Mars Atmosphere Modeling and Observations.
[11] Wang, H. and Richardson, M. I. (2015) Icarus, 251, doi: 10.1016/J.ICARUS.2013.10.033
[12] Cantor, B. A. et al. (2010) Icarus, 208, doi: 10.1016/j.icarus.2010.01.032
[13] Cantor, B. A. et al. (2018), Icarus, 321, doi: 10.1016/j.icarus.2018.10.005
[14] Heavens, N. G. et al. (2015) GRL, 42(10), doi: 10.1002/2015GL064004
[15] Chaffin, M. S. et al. (2021) Nat. Astronomy, 5(10) doi: 10.1038/s41550-021-01425-w